Received: 19 January 2021 | Revised: 20 April 2021 | Accepted: 1 May 2021

DOI: 10.1111/bcp.14977

ORIGINAL ARTICLE

Multiparametric magnetic resonance imaging to characterize cabotegravir long-acting formulation depot kinetics in healthy adult volunteers

Beat M. Jucker[1] | Edward J. Fuchs[2] | Sarah Lee[3] | Valeriu Damian[1] | Paul Galette[1] | Robert Janiczek[1] | Katarzyna J. Macura[2] | Michael A. Jacobs[2] | Ethel D. Weld[2] | Meiyappan Solaiyappan[2] | Ronald D'Amico[4] | Jafar Sadik Shaik[1] | Kalpana Bakshi[1] | Kelong Han[1] | Susan Ford[5] | David Margolis[4] | William Spreen[4] | Manish K. Gupta[1] | Craig W. Hendrix[2] | Parul Patel[4]

[1]GlaxoSmithKline, Collegeville, PA, USA

[2]Departments of Internal Medicine and Radiology, The Johns Hopkins School of Medicine, Baltimore, MD, USA

[3]Amallis Consulting Ltd, London, UK

[4]ViiV Healthcare, Research Triangle Park, NC, USA

[5]GlaxoSmithKline, Research Triangle Park, NC, USA

Correspondence
Beat M. Jucker PhD, Bioimaging, Department In Vitro/In Vivo Translation, 1250 S Collegeville Rd, Collegeville, PA 19426, USA.
Email: beat.m.jucker@gsk.com

Funding information
ViiV Healthcare

Aim: Cabotegravir long-acting (LA) intramuscular (IM) injection is being investigated for HIV preexposure prophylaxis due to its potent antiretroviral activity and infrequent dosing requirement. A subset of healthy adult volunteers participating in a Phase I study assessing cabotegravir tissue pharmacokinetics underwent serial magnetic resonance imaging (MRI) to assess drug depot localization and kinetics following a single cabotegravir LA IM targeted injection.

Methods: Eight participants (four men, four women) were administered cabotegravir LA 600 mg under ultrasonographic-guided injection targeting the gluteal muscles. MRI was performed to determine injection-site location in gluteal muscle (IM), subcutaneous (SC) adipose tissue and combined IM/SC compartments, and to quantify drug depot characteristics, including volume and surface area, on Days 1 (≤2 hours postinjection), 3 and 8. Linear regression analysis examined correlations between MRI-derived parameters and plasma cabotegravir exposure metrics, including maximum observed concentration (C_{max}) and partial area under the concentration–time curve (AUC) through Weeks 4 and 8.

Results: Cabotegravir LA depot locations varied by participant and were identified in the IM compartment ($n = 2$), combined IM/SC compartments ($n = 4$), SC compartment ($n = 1$) and retroperitoneal cavity ($n = 1$). Although several MRI parameter and exposure metric correlations were determined, total depot surface area on Day 1 strongly correlated with plasma cabotegravir concentration at Days 3 and 8, C_{max} and partial AUC through Weeks 4 and 8.

Beat M. Jucker and Edward J. Fuchs are joint first authors and contributed equally to the manuscript.

The authors confirm that the PI for this paper is Craig Hendrix, MD and that he had direct clinical responsibility for patients.

Conclusion: MRI clearly delineated cabotegravir LA injection-site location and depot kinetics in healthy adults. Although injection-site variability was observed, drug depot surface area correlated with both plasma C_{max} and partial AUC independently of anatomical distribution.

KEYWORDS
antiretrovirals, cabotegravir, HIV/AIDS, MRI, pharmacokinetics-pharmacodynamic

1 | INTRODUCTION

Cabotegravir long-acting (LA) parenteral is a promising HIV-1 integrase strand transfer inhibitor candidate for HIV preexposure prophylaxis due to its potent antiretroviral activity and infrequent dosing requirements.[1] Cabotegravir, which has a plasma half-life of ~21–50 days when administered as an LA parenteral, demonstrated protective antiviral activity in rectal and vaginal nonhuman primate simian immunodeficiency virus and HIV-challenge models.[2,3] Cabotegravir concentrations achieved in anatomical mucosal tissue sites associated with sexual HIV transmission following an intramuscular (IM) dose of preexposure prophylaxis in humans are unknown. This study is part of a Phase I study that assessed tissue compartmental pharmacokinetic (PK) analysis of cabotegravir LA (ClinicalTrials.gov Identifier: NCT02478463). It included a 4-week oral dose lead-in to assess tolerability, a washout period of 14–42 days, and a single 600 mg dose of cabotegravir LA administered as a single 3 mL intragluteal injection under ultrasonographic guidance. Postinjection PK sampling of blood plasma; vaginal, cervical, and rectal tissues; and cervicovaginal and rectal fluids over 12 weeks was performed. A subset of participants underwent magnetic resonance imaging (MRI) as an exploratory objective to serially assess evolution of the injection depot for 1 week following administration.

Long-acting injectables have been clinically used to sustain therapeutic drug levels at a target site to reduce the frequency of dosing required.[4,5] Despite development of clinically available LA injectables,[6,7] questions remain about mechanisms that control drug release from the depot site, including impact of physiochemical characteristics (e.g., solubility, particle size, particle charge) on dissolution and influence of biologic factors, including depot size, shape, anatomical location, inflammatory response, perfusion and pH.[8] Significant plasma PK variability was noted in prior cabotegravir LA studies,[9–11] with potential factors contributing to this variability, including administration technique (i.e., injection into subcutaneous [SC] fat *vs* gluteal muscle) or dose volume (i.e., split *vs* unsplit injections).

In preclinical experiments, MRI was used to noninvasively identify drug depot location, volume and surface area changes in IM and SC locations following cabotegravir LA administration in rats.[12] Although ultrasonography is used widely for guidance of LA drug delivery and can be used to assess depot characteristics,[13,14] few reports use MRI to visualize IM injections or quantitatively characterize LA drug depot.

What is already known about this subject

- As an intramuscular injection, long-acting (LA) cabotegravir is promising for HIV-1 preexposure prophylaxis given its potent antiretroviral activity and infrequent dosing requirements
- Pharmacokinetic (PK) variability has been observed following cabotegravir LA injection in healthy individuals, but characterization of cabotegravir LA drug depot kinetics is limited to preclinical models

What this study adds

- Magnetic resonance imaging of cabotegravir LA injection depot location demonstrated high deposition variability between participants despite ultrasonographic-guided administration
- Cabotegravir LA total depot surface area strongly correlated with plasma exposure metrics, independent of anatomical distribution
- These results help to better explain the observed PK variability associated with cabotegravir LA injection

Yet, injectable drug depot characteristics were identified, including inflammation and persistence, since the early clinical use of MRI.[15,16] Therefore, this exploratory substudy was designed to investigate use of MRI to clinically image the evolution of the cabotegravir LA injection depot and examine the depot morphometry and its relationship to plasma concentrations and noncompartmental analysis-derived plasma exposure metrics.

In this Phase I study, four men and four women were enrolled in an imaging substudy and underwent noncontrast-enhanced MRI following cabotegravir LA injection (Day 1) on Day 3 and on Day 8 to measure the injection depot following a single cabotegravir 600 mg IM targeted dose. Magnetic resonance imaging was performed ≤2 hours following injection (Day 1) and at Days 3 and 8 postinjection for morphometric assessment (i.e., volume, surface area), transverse relaxation time constant (T2) and apparent diffusion coefficient (ADC) quantification of the depot evolution.

2 | METHODS

Magnetic resonance imaging was performed on a cohort of healthy volunteers enrolled into a Phase I open-label study designed to assess the PK of cabotegravir LA in plasma, tissues and mucosal secretions associated with HIV-1 transmission following a single 600 mg IM targeted injection. The MRI substudy enrolled eight healthy participants without HIV-1 infection (four men, four women; Table 1). The study consisted of a screening period, a 28-day oral cabotegravir lead-in phase at a dose of 30 mg day^{-1} followed by a 14- to 42-day washout period to accommodate flexibility in clinic scheduling, and a single 3 mL IM dose of cabotegravir LA 600 mg (200 mg mL^{-1} cabotegravir dose concentration; Figure 1). Following dosing, participants returned for safety assessments and PK sampling of the blood plasma periodically through Weeks 12, 24 and 36 postinjection, with a follow-up visit at Week 52 postinjection (Figure 1).

After the oral cabotegravir washout period, each participant received the cabotegravir IM dose into the ventrogluteal muscle compartment under ultrasonographic-guided administration using a Z-tracking technique. A ≥9 cm spinal needle was used to ensure drug deposition occurred within the ventrogluteal muscle rather than SC tissue, which, at times, may occur using standard 1.5-inch needles. Noncontrast-enhanced MRI was performed on participants on Days 1 (≤2 hours postdose), 3 and 8 (see Supplemental Information). Quantitative assessments of volume, surface area, T2 and ADC of the drug depot were performed. The drug depot volume (mL) and surface area (mm^2) were measured in individual (i.e., gluteal muscle, SC adipose tissue) and combined (i.e., IM and SC) compartments defined as total depot. The drug depot volume and surface area were measured in the retroperitoneal (RP) cavity in one participant who received a misinjection.

Plasma cabotegravir PK samples were collected at the following timepoints: Days 1 (4 h), 3 (48 h), 5 (96 h) and 8 (168 h); Weeks 4, 8, 12, 24, 36 and 52; and concentrations were determined using high-performance liquid chromatography with tandem mass spectrometry.[17] Magnetic resonance imaging was performed immediately after cabotegravir injection and before the 4-hour blood plasma PK assessment on Day 1 and within 2 hours of PK assessment on Days 3 and 8. Pharmacokinetic analysis of drug concentrations was performed by noncompartmental analysis using the linear up and log down application of the trapezoidal rule for model 200 (extravascular administration) of WinNonlin software version 6.3 or higher (Certara, Princeton, NJ).

Linear regression analysis was used to determine the relationship between plasma cabotegravir concentrations at Days 1, 3 and 8, plasma exposure metrics and cabotegravir LA depot-derived MRI parameters. As no prespecified statistical hypothesis was tested, an arbitrary correlation threshold of 0.7 was used in analyses where all eight participant values were used (e.g., total depot volume, surface area), 0.8 when only six participant values were used (e.g., IM depot volume, surface area), and 0.9 when only five participant values were used (e.g., SC tissue depot volume, surface area). All figures derived from MRI parameters and exposure metrics were generated using GraphPad Prism version 8.1.2 (GraphPad Software, San Diego, CA).

The study was conducted at Johns Hopkins Hospital (Baltimore, MD) in accordance with the International Conference on Harmonisation of Technical Requirements for Registration of Pharmaceuticals for Human Use Good Clinical Practice and the principles of the Declaration of Helsinki. Johns Hopkins Medicine Institutional Review Board (Baltimore, MD) approved the study protocol and conduct. All participants provided written informed consent. This study was sponsored by ViiV Healthcare.

2.1 | Nomenclature of targets and ligands

Key protein targets and ligands in this article are hyperlinked to corresponding entries in http://www.guidetopharmacology.org, and are permanently archived in the Concise Guide to PHARMACOLOGY 2019/20.[18]

3 | RESULTS

Body mass indices (BMIs) of participants were between 21.4 and 33.1 kg m^{-2} with male and female mean (range) BMIs equal to 26.2 (21.4–29.2) and 30.2 (26.1–33.1) kg m^{-2}, respectively (Table 1). Additional participant demographics are shown in Table 1. No serious

TABLE 1 Demographics of participants and injection-site location as determined by MRI

Participant	Sex	Age, years	Height, cm	Weight, kg	BMI, kg/m^2	Injection-site location
1	F	43	172	89.9	30.4	RP
2	F	27	155	74.6	31.1	IM/SC
3	F	44	157	81.6	33.1	IM
4	F	31	170	75.5	26.1	IM
5	M	29	170	73	25.3	SC
6	M	43	178	91.6	28.9	IM/SC
7	M	25	188	75.8	21.4	IM/SC
8	M	35	184	98.9	29.2	IM/SC

BMI, body mass index; F, female; IM, intramuscular; M, male; MRI, magnetic resonance imaging; RP, retroperitoneal; SC, subcutaneous.

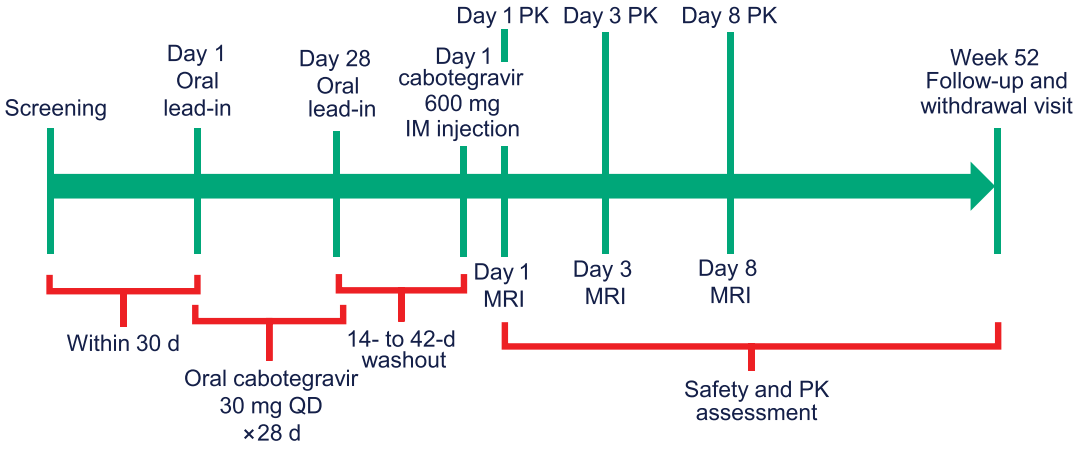

FIGURE 1 Study protocol illustrating cabotegravir oral dose lead-in (30 mg day^{-1}), washout, cabotegravir LA (600 mg) gluteal muscle-targeted injection and PK assessment visits and follow-up. MRI was performed on Days 1 (≤2 h postinjection), 3 and 8. IM, intramuscular; LA, long acting; MRI, magnetic resonance imaging; PK, pharmacokinetics; QD, once daily

adverse events were identified during the MRI period of the substudy. Each of the eight participants underwent MRI, including spin-echo T2-weighted, T2 mapping, Dixon and diffusion-weighted imaging acquisitions, except for participant 1, who did not have diffusion-weighted imaging acquisition on Day 1. All acquired imaging data passed quality control in which images were visually reviewed for any artifacts as well as gross movement, and were analysed. Serial MRI was performed to identify the cabotegravir LA depot location, depot morphometry (e.g., volume, surface area), and evolution of the depot over the initial study week postinjection. Although cabotegravir LA injection was performed under ultrasonographic guidance, the depot location was quite variable and identified in the RP cavity in one participant, discretely in the IM tissue in two participants, in the SC tissue in one participant, and in both IM and SC tissues in the remaining four participants (Figure 2). The Dixon image was used to differentiate between SC and IM tissues and measure SC tissue thickness along the injection track (i.e., from the fiduciary marker to the depot; Figure 2A). Increases in depot shape and volume observed in the RP cavity, IM alone, SC alone and combined IM and SC depot locations during the one-week postinjection imaging period reflect depot expansion, potentially due to both drug and inflammatory infiltrates (Figure 2B–E). The drug depot appeared to be entirely or predominantly administered in the IM compartment, but it possibly leaked out through the needle track in the four participants administered the study drug via the IM and SC route (Figure 2E).

Both individual participant depot volume (Figure 3A) and surface area (Figure 3B) were calculated from multislice, T2-weighted MRI. These volumes and surface areas were further assessed to determine each parameter associated with RP, IM, SC, and IM and SC tissue compartments in the four participants for whom the study drug resided in both locations (Figure 3C,D). Although the cabotegravir LA dose volume was only 3 mL upon injection, within 2 hours of dosing, the mean (standard error of mean) MRI-derived depot volume increased to 29.3 (4.5) mL, with a larger increase observed in IM (∼tenfold) than in the SC or RP locations (∼three- and ∼fourfold, respectively; Figure 3C). In all but one participant (SC administration), the MRI-derived depot volume continued to increase throughout the one-week imaging period (mean [standard error of mean], 70.0 [20.1] and 147.3 [49.4] mL at Days 3 and 8, respectively). The cabotegravir LA depot in participant 5 peaked at Day 3 before resolving in SC tissue (Figure 3A,C). Calculated surface area of the entire depot showed similar growth trends to their volumes (Figure 3B,D). In addition, volume and surface area were calculated for the entire depot (i.e., IM + SC) as well as for individual IM and SC compartments in each participant (Figure 3E,F). Total surface area is generally less than the sum of the individual IM and SC surface areas, because the surface area of the interface between IM and SC depot components is not included in the measurement of total depot surface area.

Both individual participant T2-weighted and ADC MRI parameters were quantified to determine if any unique physiologic characteristics to the depot could be identified (e.g., differentiating drug *vs* leukocyte infiltration; Figure 4A,B). In addition, investigating the depot heterogeneity using these measurements could be of value to detect drug agglomeration *vs* diffuse localization. Mean T2 values were lower in IM than in SC tissue compartments on Day 1, and a slight reduction in this parameter value was observed in both locations by Day 3 that was maintained through Day 8 (Figure 4C). Conversely, ADC values were lower in SC than IM tissue on Day 1, and the SC depot ADC value dropped by Day 3 and was maintained at this level until Day 8 (Figure 4D).

Following the oral cabotegravir washout period, baseline cabotegravir concentrations were below detectable limits. Following gluteal muscle-targeted cabotegravir LA administration, all participants exhibited a rapid increase in plasma cabotegravir exposure, with maximum concentration (C_{max}) occurring between 51 and 170 hours for six of eight participants; however, two participants (participants 1 and 5), one of whom was a woman with a BMI > 30 kg m^{-2}, had significantly longer time of maximum observed concentration (T_{max}) of 505 and 1252 hours, respectively (Table 2; Figure 5A). Plasma

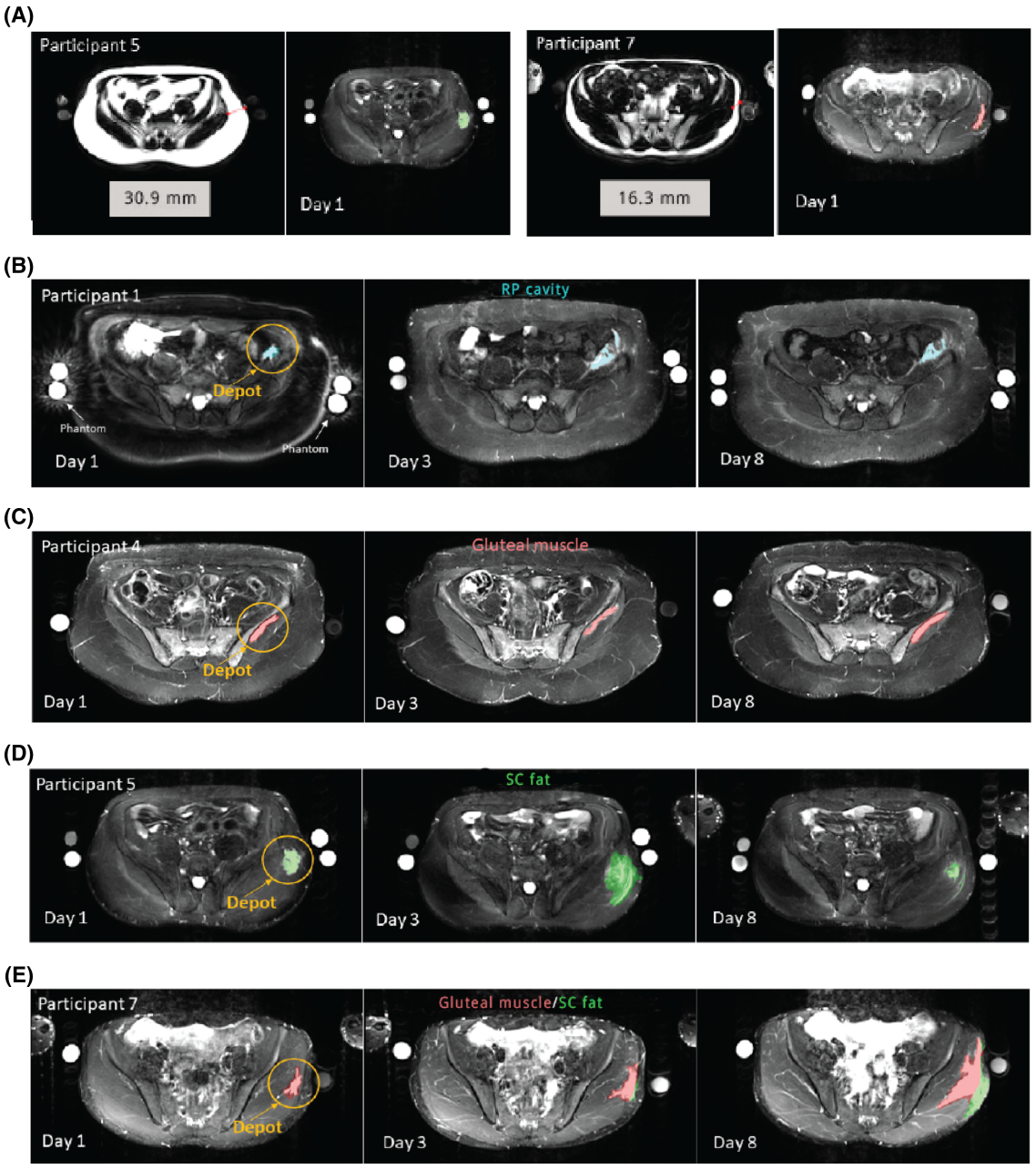

FIGURE 2 Temporal MRI of cabotegravir LA depots in representative sites. (A) SC adipose tissue thickness (red line) along the needle track varied greatly in participants. Ultrasonographic-guided cabotegravir LA injections were administered in (B) RP, (C) IM, (D) SC and (E) IM and SC locations. Each panel contains a representative image of the serial, transverse, T2-weighted slice section obtained through the same depot location on Days 1, 3 and 8. Each depot was segmented to show RP depot in blue, gluteal muscle depot in red, and SC adipose depot in green. MRI T2 reference phantoms were placed next to the participant. IM, intramuscular; LA, long acting; MRI, magnetic resonance imaging; RP, retroperitoneal; SC, subcutaneous; T2, transverse relaxation time constant

cabotegravir C_{max} was numerically higher in participants for whom the study drug was administered at the IM and IM and SC depot site *vs* the RP and SC depot site (Table 2; Figure 5B). Although partial area under the concentration–time curve (AUC) to 4 ($AUC_{0\text{-}4wk}$) or 8 weeks ($AUC_{0\text{-}8wk}$) was considerably lower in two participants with RP and SC administration routes (736–2557 h*μg mL^{-1}), overall AUC did not vary greatly between participants (mean [standard error of mean], 3737 [317] h*μg mL^{-1}). Plasma cabotegravir concentrations and exposure metrics were generally similar between men and women, with increased C_{max} and decreased overall AUC values observed in men compared with women (mean [standard error of mean], 5.485 [0.975] *vs* 3.650 [0.944] μg mL^{-1} for C_{max} and 3341 [180] *vs* 4133 [577] h*μg mL^{-1} for AUC). Plasma cabotegravir exposure during the imaging period and noncompartmental analysis-derived metrics (e.g., C_{max}, T_{max}, $AUC_{0\text{-}4wk}$, $AUC_{0\text{-}8wk}$) are shown in Table 2.

Linear regression analysis was performed to assess the relationship between the MRI-derived parameters and plasma cabotegravir

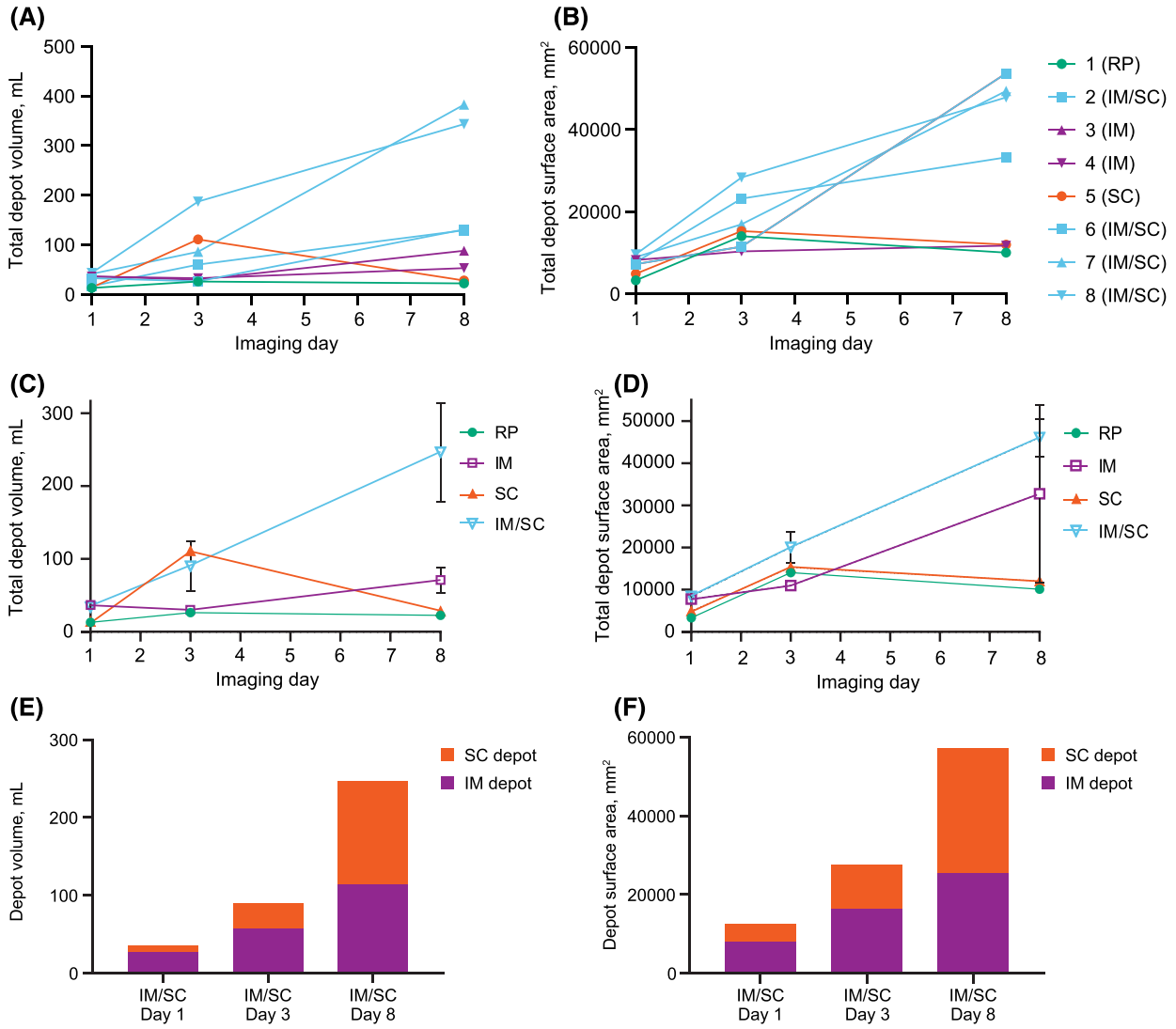

FIGURE 3 MRI-assessed cabotegravir LA depot volume and surface area. (A) Total drug depot volume and (B) surface area were measured for each participant on Days 1, 3 and 8. (C) Total drug depot volume and (D) surface area were measured in RP, IM, SC, and IM and SC tissue compartments for each participant. In those participants who received the drug administered in the IM and SC tissue compartment, both IM and SC contributions to the average (E) total depot volume and (F) surface area in these individuals were assessed. Data in panels (C) and (D) are presented as mean ± SEM. Data in panels (E) and (F) are presented as mean values for both IM and SC depots. IM, intramuscular; LA, long acting; MRI, magnetic resonance imaging; RP, retroperitoneal; SC, subcutaneous; SEM, standard error of mean

exposure metrics. Cabotegravir LA depot volumes and surface area (total [IM + SC] and IM and SC tissue individually) correlations with Day 1, 3 and 8 plasma cabotegravir concentrations, C_{max}, T_{max}, $AUC_{0\text{-}4wk}$ and $AUC_{0\text{-}8wk}$ were derived, and several positive and negative correlations were observed (Table 3; Figure 6A,B). Interestingly, total depot surface area strongly correlated with several exposure metrics, including cabotegravir plasma C_{max} and $AUC_{0\text{-}8wk}$ (Table 3; Figure 6A). Although a trend towards positive correlations was also observed between total depot volume with cabotegravir exposure metrics, this trend was not as strong as with the total depot surface area. The stronger relationship between PK and depot surface area *vs* PK and depot volume is consistent with the Noyes–Whitney equation, which expresses drug-dissolution rate as a function of surface area.[19] When examining the relationship between IM or SC depot volume and surface area with cabotegravir exposure metrics, only IM volume and surface area at Day 1 positively correlated with $AUC_{0\text{-}4wk}$ ($r = 0.77$ and 0.78 respectively; Table 3), whereas Day 1 SC depot volume negatively correlated with Day 3 and 8 cabotegravir PK ($r = -0.78$ and -0.72 respectively; Table 3). Interestingly, several negative correlations were observed between T2-weighted MRI parameters and cabotegravir exposure metrics (Table 3; Figure 6B); however, the T2 values for both RP and SC tissue depots were considerably higher than that observed in the IM depot at Day 1 (Figure 4C). Therefore, these high values skewed the correlations. No correlations were observed between total depot ADC values and cabotegravir exposure metrics.

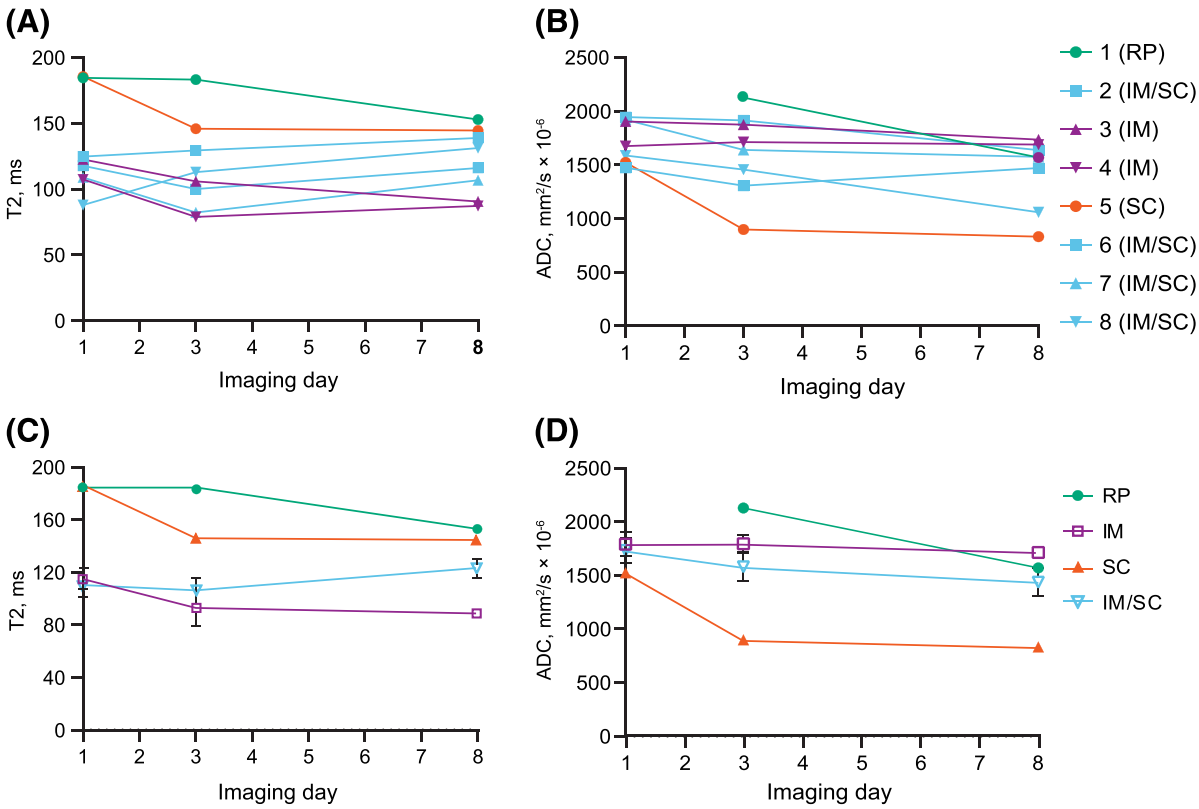

FIGURE 4 MRI-assessed cabotegravir LA depot mean T2 and mean ADC parameters. (A) Total drug depot mean T2 and (B) mean ADC were measured for each participant on Days 1, 3 and 8. (C) Total drug depot mean T2 and (D) mean ADC were measured in RP, IM, SC, and IM and SC tissue compartments for each participant. Data in panels (C) and (D) are presented as mean ± SEM. On Day 1 in participant 1, RP ADC was not measured. ADC, apparent diffusion coefficient; IM, intramuscular; LA, long acting; MRI, magnetic resonance imaging; RP, retroperitoneal; SC, subcutaneous; SEM, standard error of mean; T2, transverse relaxation time constant

TABLE 2 Plasma cabotegravir concentrations and exposure metrics for each participant

	Plasma cabotegravir							
Participant	Day 1 µg/mL	Day 3	Day 8	C_{max}	T_{max} h	$AUC_{0\text{-}4Wk}$ h*µg/mL	$AUC_{0\text{-}8Wk}$	AUC_{Last}
1	0.135	0.664	1.100	1.260	505	736	1513	4697
2	0.270	2.130	3.600	3.600	170	2024	3063	3346
3	0.893	5.870	5.250	5.870	51	2258	2829	3013
4	0.276	3.500	3.560	3.870	93	2250	3801	5475
5	0.109	0.723	1.010	3.060	1252	853	2557	3526
6	0.323	3.030	4.740	7.030	96	2163	2712	2810
7	0.290	3.250	4.700	4.750	97	2192	3058	3592
8	0.234	3.830	4.950	7.100	97	2336	3169	3435

AUC, area under the concentration–time curve; AUC_{Last}, AUC to final time point; C_{max}, maximum concentration; T_{max}, time to maximum concentration.

4 | DISCUSSION

This study was performed to define the injection-site depot location and examine depot morphometry and multiparametric MRI characteristics during the initial week following an IM-targeted cabotegravir LA injection. Variability in PK was previously observed with cabotegravir LA IM administration in healthy participants when administered free-hand using a standard 1.5-inch needle, and this variability could only partially be associated with sex or BMI.[9,20] Therefore, the current study examined injection-site variability and drug depot volume and surface area as well as their relationship to cabotegravir plasma exposure metrics. Although injection-site variability was observed, total

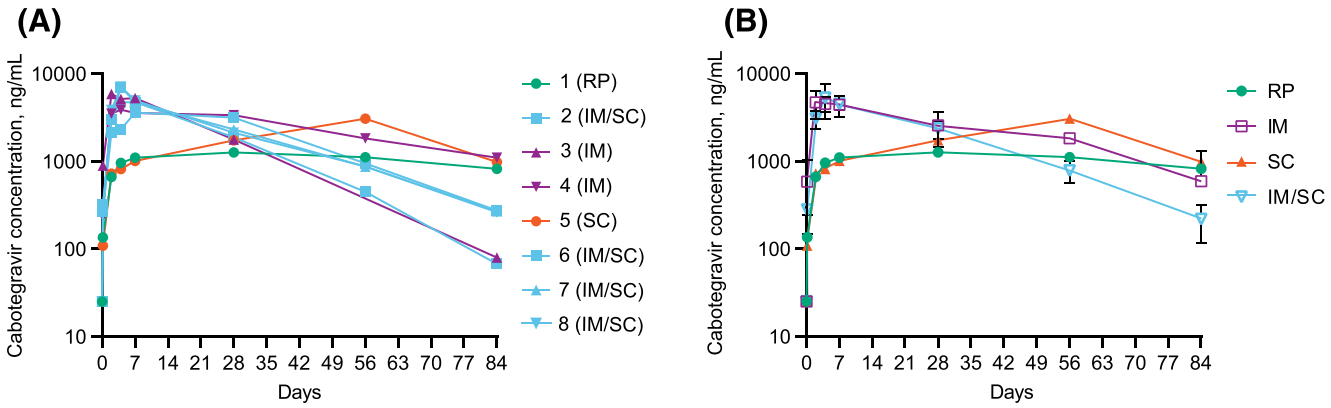

FIGURE 5 Plasma cabotegravir pharmacokinetics profile. (A) Plasma cabotegravir concentration is shown for each imaging participant out to 84 days after cabotegravir LA administration. (B) Mean plasma cabotegravir concentration is shown for depot location. IM, intramuscular; LA, long acting; RP, retroperitoneal; SC, subcutaneous. Data in panel (B) are presented as mean ± standard error of mean

TABLE 3 Correlations derived from linear regression analysis of MRI-derived cabotegravir parameters with plasma cabotegravir concentrations and exposure metrics

Variable	Day 1	Day 3	Day 8	C_{max}	T_{max}	$AUC_{0\text{-}4Wk}$	$AUC_{0\text{-}8Wk}$
SC thickness	0.61	0.48	0.22	0.15	−0.34	0.20	−0.01
Total depot volume (Day 1)	0.38	0.71	0.74	0.48	−0.66	0.80	0.73
Total depot surface area (Day 1)	0.31	0.73	0.89	0.80	**−0.70**	0.94	0.83
IM depot volume (Day 1)	0.23	0.60	0.32	0.01	−0.62	0.77	0.43
IM depot surface area (Day 1)	−0.27	0.20	0.37	0.35	−0.47	0.78	0.32
SC depot volume (Day 1)	−0.51	−0.78	−0.72	−0.65	0.55	−0.60	−0.52
SC depot surface area (Day 1)	−0.19	−0.59	−0.47	−0.59	0.24	−0.32	−0.23
Total depot T2 (Day 1)	−0.33	**−0.75**	**−0.91**	**−0.77**	0.83	**−0.97**	**−0.78**
Total depot ADC (Day 1)	0.55	0.59	0.63	0.54	−0.48	0.45	−0.15
Total depot volume (Day 3)	−0.31	0.02	0.15	0.46	0.17	0.11	0.17
Total depot surface area (Day 3)	−0.18	0.12	0.37	0.69	−0.15	0.25	−0.01
IM depot volume (Day 3)	−0.34	0.07	0.56	0.69	−0.30	0.65	−0.09
IM depot surface area (Day 3)	−0.14	0.13	0.69	0.91	−0.43	0.52	−0.40
SC depot volume (Day 3)	−0.89	−0.35	−0.56	−0.16	0.69	−0.59	−0.22
SC depot surface area (Day 3)	−0.59	0.10	−0.13	0.08	0.24	−0.12	0.31
Total depot T2 (Day 3)	−0.37	**−0.71**	**−0.78**	−0.65	0.61	**−0.87**	**−0.86**
Total depot ADC (Day 3)	0.34	0.30	0.25	0.05	−0.58	0.14	−0.30
Total depot volume (Day 8)	−0.02	0.35	0.62	0.55	−0.46	0.56	0.35
Total depot surface area (Day 8)	−0.05	0.20	0.58	0.47	−0.48	0.56	0.34
IM depot volume (Day 8)	−0.05	−0.07	0.36	0.03	−0.15	−0.08	−0.34
IM depot surface area (Day 8)	−0.10	−0.15	0.38	0.12	−0.07	−0.16	−0.46
SC depot volume (Day 8)	0.11	0.72	0.55	0.45	−0.45	0.55	0.80
SC depot surface area (Day 8)	0.29	0.44	0.43	−0.03	−0.56	0.57	0.93
Total depot T2 (Day 8)	−0.67	**−0.82**	−0.67	−0.46	0.60	**−0.73**	−0.67
Total depot ADC (Day 8)	0.52	0.45	0.41	0.05	**−0.71**	0.41	0.08

Positive correlations that are ≥0.9 for SC depot ($n = 5$), ≥0.8 for IM depot ($n = 6$), and ≥0.7 for total depot ($n = 8$) are highlighted in green, and negative correlations that are ≤−0.9 for SC depot ($n = 5$), ≤−0.8 for IM depot ($n = 6$), and ≤−0.7 for total depot ($n = 8$) are highlighted in red. SC thickness is measured along the injection track, i.e., from the fiduciary marker to the drug depot. ADC, apparent diffusion coefficient; AUC, area under the concentration-time curve; C_{max}, maximum concentration; IM, intramuscular; SC, subcutaneous; T2, transverse relaxation time constant; T_{max}, time to maximum concentration.

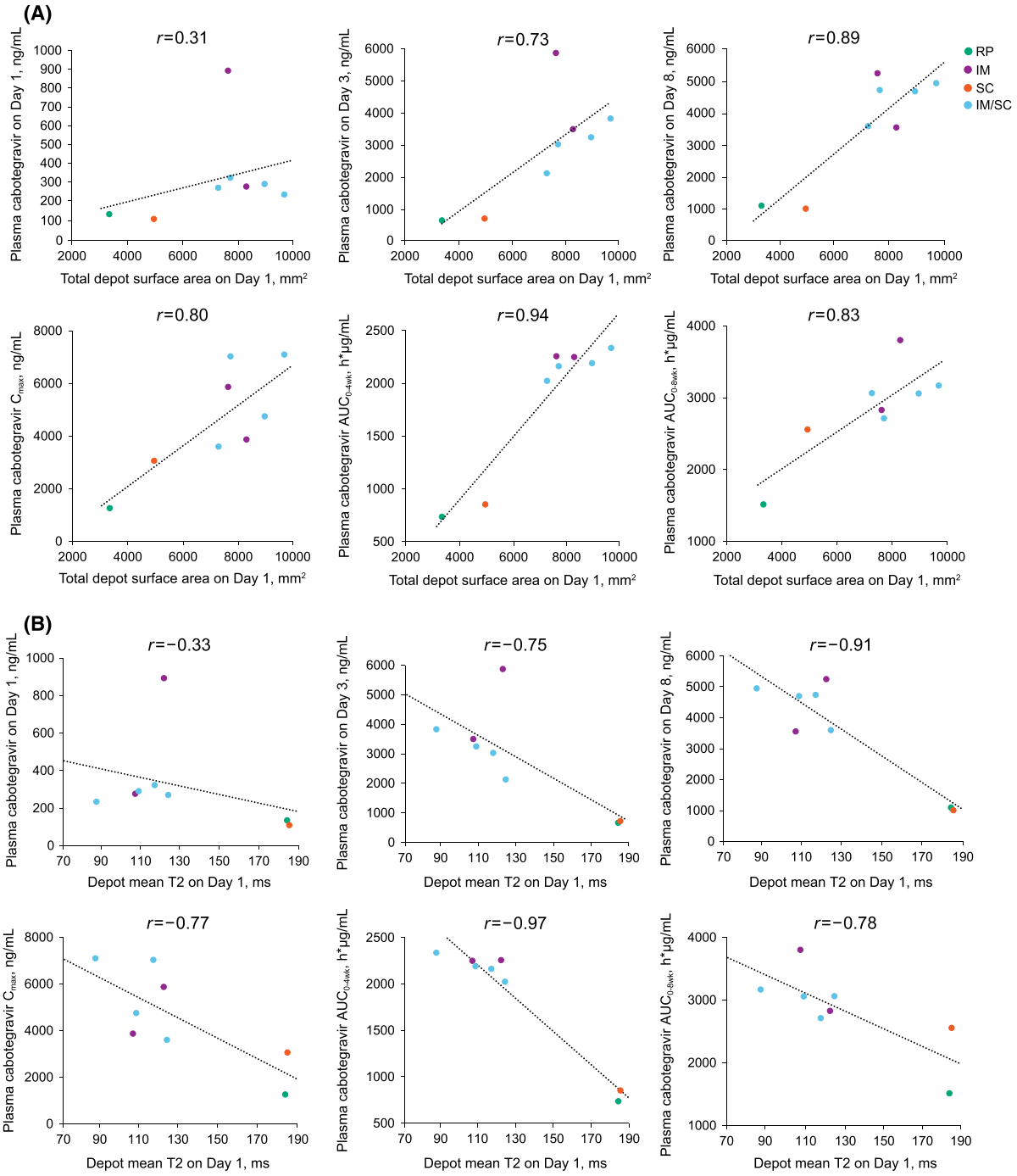

FIGURE 6 Linear regression analysis performed on cabotegravir exposure metrics and MRI-derived parameters. The strongest positive correlations between plasma cabotegravir concentrations (Days 1, 3 and 8) and exposure metrics (C_{max}, $AUC_{0\text{-}4wk}$, $AUC_{0\text{-}8wk}$) and MRI-measured cabotegravir LA depot volume, surface area, T2 and ADC parameters were with (A) total depot surface area observed on Day 1. Conversely, the strongest negative correlations between plasma cabotegravir concentrations and exposure metrics and MRI-measured cabotegravir LA depot volume, surface area, T2, and ADC parameters were with (B) T2 observed on Day 1. ADC, apparent diffusion coefficient; AUC, area under the concentration–time curve; C_{max}, maximum concentration; LA, long acting; MRI, magnetic resonance imaging; T2, transverse relaxation time constant

depot surface area measured following cabotegravir LA administration (Day 1) appeared to strongly correlate with both plasma C_{max} and partial AUC independent of injection-site location. Additional MRI parameter assessments (T2-weighted and ADC) were less informative about physiologic changes, drug agglomeration processes, or both occurring during the assessed timeframe. Although complex physiologic processes are known to occur following IM administration of LA injectables, including slow dissolution of the drug substance, local acute

and chronic inflammation, angiogenesis and lymph drainage,[21,22] the morphometric data obtained in the present study may nevertheless be used to build complex pharmacometric, multicompartment models that may inform future clinical trial simulations and study design optimization. However, because the sample size of the present study is small and no imaging was performed in previous cabotegravir clinical studies, correlation of the larger clinical dataset based on variable anatomical injections is not possible.[23–25]

This study revealed some unexpected findings, including variable cabotegravir LA depot injection-site location, considering that drug administration was performed under ultrasonographic guidance. However, these findings may be unsurprising considering that previous studies have shown that success rates of intended IM injections vary (~32–52%), with the rest potentially resulting in inadvertent SC drug deposition.[26] Preclinical studies of a similar LA injectable also demonstrated that the injection volume may reside in the SC compartment despite employing ultrasonographic guidance.[27] In the present study with its small sample size, no relationship was observed between injection-site location (i.e., SC, IM, RP) and either sex or BMI, and no serious adverse events associated with the variable injection-site locations were reported. In fact, the participant who had the most significant SC adipose tissue thickness along the needle track for cabotegravir LA administration (73.5 mm) was injected entirely in the IM space, whereas the participant who received a discrete depot administration in the SC location had a less-than-average SC adipose tissue thickness (30.9 mm) along the needle track. In this participant, ultrasonography of the SC layer suggested that the adipose tissue thickness was <30.9 mm; structurally, it had the appearance of pseudofat (estimated thickness ~10 mm). These observations contrast with findings from studies investigating variables associated with antipsychotic LA administration, wherein an increased risk of injection failure was associated with female sex, obesity, site of injection and SC fat depth.[26,28] However, needle track-associated retrograde drug spillage of cabotegravir LA into the SC location was observed after IM administration in some participants (e.g., participant 7; Figure 2E). In addition, the participant who was misinjected in the RP cavity exhibited a very different PK profile than the participants whose route of administration was either IM, IM and SC, or SC. The C_{max} was significantly lower (18–41%) in this participant, but the exposure duration >90% maximal inhibitory concentration (IC_{90}; 166 ng mL^{-1}) lasted for >180 days, whereas all other participants had significantly lower cabotegravir concentrations, i.e., below IC_{90} at 180 days (data not shown), possibly reflecting a lower absorption rate in RP *vs* IM compartments. However, although this participant exhibited a rather slow absorption rate and a long T_{max} of ~28 days, the one participant discretely administered into the SC space, where blood flow and absorption are typically reduced,[26,28] had a T_{max} of ~56 days. Because cabotegravir has low water solubility and high membrane permeability,[9] its rates of dissolution and absorption are expected to be a function of depot surface area.[19] The dissolved amount of cabotegravir will be higher with increased volume of interstitial fluid and thus, associated with an increased level of inflammation.[9] At Day 8, the depot volume and inflammation level were the lowest for SC and RP injections, an observation that may explain the longer T_{max}. However, because of the small sample size in this study, definitive PK conclusions with respect to anatomical site are limited.

Noninvasive imaging approaches to assess LA drug distribution in humans for durations of weeks to months have been sparingly applied, because detection techniques to directly assess drug substance are not readily available.[29–33] Computed tomography has been used to assess LA injectable depot location variability between gluteal muscle and SC adipose fat and, in doing so, has been used to determine the association between BMI and IM misinjections.[28,34] Ultrasonography has traditionally been used to guide injectable therapies to the intended locations and has also been used in conjunction with elastography to characterize the dispersion and physiochemical properties of the drug.[13,14] Although MRI cannot be used to visualize the active drug substance in a solid-suspension formulation like cabotegravir LA, traditional excipients (e.g., oil, polyethylene glycol, mannitol, water) generate adequate MRI signal for detection and discrimination from biologic tissue-based signal.[30,32,35] Magnetic resonance imaging was also used to assess drug depot volume expansion in a patient receiving an intragluteal injection of diclofenac 2 mL in which a rapid increase in depot volume over the initial 24 hours was observed.[33] In a previous rodent imaging study, cabotegravir LA IM depots appeared to manifest a subacute inflammatory response caused by the active drug particles that led to increased oedema in the depot region, thereby resulting in additional high-intensity MRI signal.[12] Although the drug depot volume also increased in the SC-administered animals, the expansion observed in these animals was less than that observed for IM administration. Interestingly, the vehicle-administered depot volume appeared to quickly decrease below baseline, reflecting rapid dissipation of the excipients from the depot region and minimal oedema in the absence of drug substance. Our findings of cabotegravir LA drug being distributed along IM fascial planes is consistent with previous clinical observations and with our previous preclinical MRI study findings, which were confirmed using imaging mass spectroscopy showing cabotegravir LA drug colocated within interfacial planes of muscles.[12,31,33]

When examining which key imaging endpoints (e.g., volume, surface area, T2-weighted, ADC) were key markers associated with drug absorption and PK exposure, the drug depot surface area assessed within 2 hours of administration was highly correlated with early plasma cabotegravir PK, C_{max} and with partial $AUC_{0\text{-}4wk}$. This is unsurprising because insoluble drug particle dissolution rates are directly related to specific surface area of the drug particle,[36,37] and dissolution studies showing surface area of insoluble drugs used as LA injectables correlated well with in vivo drug exposure.[21,38] However, in addition to drug particle size or surface area driving dissolution, the increased surface area of the depot has been shown to be associated with increased C_{max} and AUC when administering two cabotegravir LA depots instead of a single depot to healthy volunteers.[9] Although all participants were administered the identical 3-mL volume in the present study, independent of injection-site location, the depot surface area rapidly increased during the first week postdose, perhaps reflecting less agglomeration and resulting in increased particle

surface area exposure. Although total depot volume on Day 1 showed similar trends regarding correlations with early exposure metrics, these relationships were not as strong as with the total depot surface area on Day 1, suggesting that the shape of the depot could be irregular (Figure 2D) and exhibit a greater surface area by volume ratio than theoretically possible assuming a spherical drug deposition. When examining relationships between IM and SC depot surface area or volume and plasma cabotegravir exposure metrics, there was less statistical power in the analysis given the fewer data points. However, although IM depot volume and surface area on Day 1 positively correlated with partial $AUC_{0\text{-}4wk}$, the SC contribution to the depot volume and surface area tended to negatively correlate with exposure metrics at this early time point. These disparate findings between IM and SC may suggest the ideal location for cabotegravir LA depot is in muscle as intended. Correlations between IM and SC depot volume and surface area and exposure metrics were lost after Day 1, possibly reflecting the depot size and shape being driven more by drug substance at Day 1, rather than by retrograde drug leak and oedema resulting from local subacute inflammatory response, which was more prevalent at later time points.

T2-weighted and ADC MRI parameters were assessed to examine whether they could differentiate between physiochemical agglomeration of drug substance and physiologic subacute inflammation. Although these MRI-derived parameter assessments have been used previously to examine drug dissolution ex vivo, no reports exist of these applications for in vivo assessment of LA injectable properties.[39,40] If drug agglomeration occurred during the initial week post-injection, then either patterns of reduced T2 and ADC or an overall reduction in these values might have been detected. Nevertheless, no patterns or regions of significance were observed in T2 or ADC change in the images, and this was also reflected in the quantitative T2 and ADC values measured in total and IM and SC regional depots. Differences existed in T2 between IM and SC depot locations as expected given that endogenous T2 values are higher in SC than IM tissue.[41] For example, the total depot T2 in participant 8 increased over time, simply reflecting the larger contribution of the SC compartment throughout the imaging week. Alternatively, ADC values tend to be higher in IM than SC tissue,[42] so total depot ADC in the same participant decreased over time. The strong negative correlations between Day 1 total depot T2 values and exposure metrics are due to the significantly higher T2 in both SC and RP depots, which were also associated with lower cabotegravir LA drug levels at this time.

MRI was used to clearly delineate injection-site location and assess cabotegravir LA depot kinetics. Although injection-site variability was associated with the current study, surface area of the cabotegravir LA depot appeared to strongly correlate with both plasma C_{max} and partial AUC independently of anatomical distribution. Imaging has potential for interrogating the physiological processes involved in LA drug depot formation and its evolution. These imaging data may help inform the development of LA therapeutics and how to optimize LA injectable physicochemical properties, including drug substance particle size distribution and LA injectable formulation variables, such as selection of excipients (i.e., surfactants, stabilizers).

ACKNOWLEDGEMENTS

Editorial assistance was provided under the direction of the authors by Megan Schmidt, PhD, and Sherri Damlo, ELS, MedThink SciCom, and funded by ViiV Healthcare. We thank Rebecca DeMoor, GlaxoSmithKline, for providing statistical guidance for this study. This study was sponsored by ViiV Healthcare.

COMPETING INTERESTS

B.M.J., V.D., P.G., R.J., J.S.S., K.B., K.H., S.F. and M.K.G. are employees of and own stock in GlaxoSmithKline. E.J.F. and E.D.W. received grant funding to their institution from GlaxoSmithKline. S.L. received personal fees from GlaxoSmithKline during the conduct of the study and from GE Healthcare outside of the submitted work and is an employee of Amallis Consulting. M.S. received institutional grant funding from GlaxoSmithKline. K.J.M. has received grants from GlaxoSmithKline, Siemens Healthineers, and Profound Medical. M.A.J. has received grants from GlaxoSmithKline, the National Institutes of Health, and the National Cancer Institute. R.D., D.M., W.S. and P.P. are employees of ViiV Healthcare and own stock in GlaxoSmithKline. C.W.H. received grant funding from, and has served on advisory boards for, ViiV Healthcare and GlaxoSmithKline.

CONTRIBUTORS

All authors have made substantial contributions to conception and design, or acquisition of data, or analysis and interpretation of data; been involved in drafting the manuscript or revising it critically for important intellectual content; given final approval of the version to be published; have participated sufficiently in the work to take public responsibility for appropriate portions of the content; and agreed to be accountable for all aspects of the work in ensuring that questions related to the accuracy or integrity of any part of the work are appropriately investigated and resolved.

DATA AVAILABILITY STATEMENT

Anonymized individual participant data and study documents can be requested for further research from www.clinicalstudydatarequest.com

REFERENCES

1. Andrews CD, Heneine W. Cabotegravir long-acting for HIV-1 prevention. *Curr Opin HIV AIDS*. 2015;10(4):258-263.
2. Andrews CD, Spreen WR, Mohri H, et al. Long-acting integrase inhibitor protects macaques from intrarectal simian/human immunodeficiency virus. *Science*. 2014;343(6175):1151-1154.
3. Radzio J, Spreen W, Yueh YL, et al. The long-acting integrase inhibitor GSK744 protects macaques from repeated intravaginal SHIV challenge. *Sci Transl Med*. 2015;7:270ra5.
4. Saenger PH, Mejia-Corletto J. Long-acting growth hormone: an update. *Endocr Dev*. 2016;30:79-97.
5. Wright JC, Burgess DJ. *Long Acting Injections and Implants*. New York: Springer; 2012.
6. Remenar JF. Making the leap from daily oral dosing to long-acting injectables: lessons from the antipsychotics. *Mol Pharm*. 2014;11(6):1739-1749.

7. Mobula L, Barnhart M, Malati C, et al. Long-acting, injectable antiretroviral therapy for the management of HIV infection: an update on a potential game-changer. *J AIDS Clin Res*. 2015;6:1000466.
8. Larsen C, Larsen SW, Jensen H, Yaghmur A, Ostergaard J. Role of in vitro release models in formulation development and quality control of parenteral depots. *Expert Opin Drug Deliv*. 2009;6(12):1283-1295.
9. Trezza C, Ford SL, Spreen W, Pan R, Piscitelli S. Formulation and pharmacology of long-acting cabotegravir. *Curr Opin HIV AIDS*. 2015;10(4):239-245.
10. Spreen W, Ford SL, Chen S, et al. GSK1265744 pharmacokinetics in plasma and tissue after single-dose long-acting injectable administration in healthy subjects. *J Acquir Immune Defic Syndr*. 2014;67(5):481-486.
11. Spreen WR, Margolis DA, Pottage JC Jr. Long-acting injectable antiretrovirals for HIV treatment and prevention. *Curr Opin HIV AIDS*. 2013;8(6):565-571.
12. Jucker BM, Alsaid H, Rambo M, et al. Multimodal imaging approach to examine biodistribution kinetics of cabotegravir (GSK1265744) long acting parenteral formulation in rat. *J Contr Release*. 2017;268:102-112.
13. Yasuhara Y, Hirai E, Sakamaki S, et al. Using ultrasonography in evaluating the intramuscular injection techniques used for administering drug treatments to schizophrenic patients in Japan. *J Med Invest*. 2012;59(1–2):213-219.
14. Yasuhara Y, Tanioka T, Takase K, et al. Intramuscular diffusion status of risperidone and aripiprazole long acting injectable (LAI) by ultrasonography. *Open J Psych*. 2016;6(2):165-172.
15. Huber DJ, Sumers E, Klein M. Soft tissue pseudotumor following intramuscular injection of "DPT": a pitfall in magnetic resonance imaging. *Skeletal Radiol*. 1987;16(6):469-473.
16. Resendes M, Helms CA, Fritz RC, Genant H. MR appearance of intramuscular injections. *AJR Am J Roentgenol*. 1992;158(6):1293-1294.
17. Landovitz RJ, Li S, Eron JJ, et al. Tail-phase safety, tolerability, and pharmacokinetics of long-acting injectable cabotegravir in HIV-uninfected adults: a secondary analysis of the HPTN 077 trial. *Lancet HIV*. 2020;7(7):e472-e481.
18. Alexander SPH, Kelly E, Mathie A, et al. The Concise Guide to PHARMACOLOGY 2019/20: introduction and other protein targets. *Br J Pharmacol*. 2019;176(suppl 1):S1-S20.
19. Smith BT. *Remington Education: Physical Pharmacy*. London: Pharmaceutical Press; 2015.
20. Ford SL, Chiu J, Lovern M, Spreen W, Kim J. Population PK approach to predict cabotegravir (CAB, GSK1265744) long-acting injectable doses for phase 2b. Presented at: Proceedings of the 54th Interscience Conference on Antimicrobial Agents and Chemotherapy; September 5–9, 2014; Washington, DC; Abstract H-645.
21. Owen A, Rannard S. Strengths, weaknesses, opportunities and challenges for long acting injectable therapies: insights for applications in HIV therapy. *Adv Drug Deliv Rev*. 2016;103:144-156.
22. Larsen SW, Larsen C. Critical factors influencing the in vivo performance of long-acting lipophilic solutions—impact on in vitro release method design. *AAPS J*. 2009;11(4):762-770.
23. Orkin C, Arasteh K, Górgolas Hernández-Mora M, et al. Long-acting cabotegravir and rilpivirine after oral induction for HIV-1 infection. *N Engl J Med*. 2020;382(12):1124-1135.
24. Overton ET, Richmond G, Rizzardini G, et al. Long-acting cabotegravir and rilpivirine dosed every 2 months in adults with HIV-1 infection (ATLAS-2M), 48-week results: a randomised, multicentre, open-label, phase 3b, non-inferiority study. *Lancet*. 2021;396(10267):1994-2005.
25. Swindells S, Andrade-Villanueva JF, Richmond GJ, et al. Long-acting cabotegravir and rilpivirine for maintenance of HIV-1 suppression. *N Engl J Med*. 2020;382(12):1112-1123.
26. Soliman E, Ranjan S, Xu T, et al. A narrative review of the success of intramuscular gluteal injections and its impact in psychiatry. *Biodes Manuf*. 2018;1(3):161-170.
27. Darville N, van Heerden M, Vynckier A, et al. Intramuscular administration of paliperidone palmitate extended-release injectable microsuspension induces a subclinical inflammatory reaction modulating the pharmacokinetics in rats. *J Pharm Sci*. 2014;103(7):2072-2087.
28. Chan VO, Colville J, Persaud T, Buckley O, Hamilton S, Torreggiani WC. Intramuscular injections into the buttocks: are they truly intramuscular? *Eur J Radiol*. 2006;58(3):480-484.
29. Sassa T, Suhara T, Ikehira H, et al. 19F-magnetic resonance spectroscopy and chemical shift imaging for schizophrenic patients using haloperidol decanoate. *Psychiatry Clin Neurosci*. 2002;56(6):637-642.
30. Kalicharan RW, Baron P, Oussoren C, Bartels LW, Vromans H. Spatial distribution of oil depots monitored in human muscle using MRI. *Int J Pharm*. 2016;505(1–2):52-60.
31. Probst M, Kühn JP, Scheuch E, et al. Simultaneous magnetic resonance imaging and pharmacokinetic analysis of intramuscular depots. *J Control Release*. 2016;227:1-12.
32. Kalicharan RW, Oussoren C, Schot P, de Rijk E, Vromans H. The contribution of the in-vivo fate of an oil depot to drug absorption. *Int J Pharm*. 2017;528(1–2):595-601.
33. Probst M, Kühn JP, Modeß C, et al. Muscle injury after intramuscular administration of diclofenac: a case report supported by magnetic resonance imaging. *Drug Saf Case Rep*. 2017;4(1):7.
34. Boyd AE, DeFord LL, Mares JE, et al. Improving the success rate of gluteal intramuscular injections. *Pancreas*. 2013;42(5):878-882.
35. Blunk JA, Nowotny M, Scharf J, Benrath J. MRI verification of ultrasound-guided infiltrations of local anesthetics into the piriformis muscle. *Pain Med*. 2013;14(10):1593-1599.
36. Bari H. A prolonged release parenteral drug delivery system—an overview. *Int J Pharm Sci Rev Res*. 2010;3:1-11.
37. Chu KR, Lee E, Jeong SH, Park ES. Effect of particle size on the dissolution behaviors of poorly water-soluble drugs. *Arch Pharm Res*. 2012;35(7):1187-1195.
38. Wen H, Jung H, Li X. Drug delivery approaches in addressing clinical pharmacology-related issues: opportunities and challenges. *AAPS J*. 2015;17(6):1327-1340.
39. Partridge TA, Ahmed M, Choudhary SB, et al. Application of magnetic resonance to assess lyophilized drug product reconstitution. *Pharm Res*. 2019;36(5):71.
40. Nott KP. Magnetic resonance imaging of tablet dissolution. *Eur J Pharm Biopharm*. 2010;74(1):78-83.
41. Pai A, Li X, Majumdar S. A comparative study at 3 T of sequence dependence of T2 quantitation in the knee. *Magn Reson Imaging*. 2008;26(9):1215-1220.
42. Subhawong TK, Jacobs MA, Fayad LM. Diffusion-weighted MR imaging for characterizing musculoskeletal lesions. *Radiographics*. 2014;34(5):1163-1177.

SUPPORTING INFORMATION

Additional supporting information may be found online in the Supporting Information section at the end of this article.

How to cite this article: Jucker BM, Fuchs EJ, Lee S, et al. Multiparametric magnetic resonance imaging to characterize cabotegravir long-acting formulation depot kinetics in healthy adult volunteers. *Br J Clin Pharmacol*. 2022;88(4):1655-1666. https://doi.org/10.1111/bcp.14977